Supplementary Information

Elucidation of the structural and magnetic properties of the anion-radical salt (Et-3,5-diMe-Pz)(TCNQ)$_2$

Erik Čižmár,[a*] Mariia Holub,[a‡] Daniela Šoltésová,[a] Vladimír Tkáč,[a] Petr Doležal,[b] Dominik Kriegner,[b,c] Václav Eigner,[c] Michal Dušek,[c] Dmitry Ziolkovskiy,[d] Mark W. Meisel,[a,e] and Alexander Feher [a]

[a] Institute of Physics, Faculty of Science, P.J. Šafárik University, Park Angelinum 9, 04001 Košice, Slovakia.

[b] Department of Condensed Matter Physics, Faculty of Mathematics and Physics, Charles University, Prague, Czech Republic.

[c] Institute of Physics of the Academy of Sciences of the Czech Republic, Prague, Czech Republic.

[d] Department of Chemistry, V. N. Karazin Kharkiv National University, Kharkiv, Ukraine.

[e] Department of Physics and National High Magnetic Field Laboratory, University of Florida, Gainesville, FL 32611-8440, USA.

[‡] Present address: Faculty of Physics and Applied Computer Science, AGH University of Krakow, al. A. Mickiewicza 30, 30-059 Kraków, Poland.

*erik.cizmar@upjs.sk

Table S1 Crystal data for (Et-3,5-di-Me-Pz)$(TCNQ)_2$ (**1**).

phase	**HT**	**LT**
Empirical formula	$2(C_{12}H_4N_4)$, $C_8H_{13}N_2$	$2(C_{12}H_4N_4)$, $C_8H_{13}N_2$
Formula weight	545.6	545.6
T (K)	250	95
λ (Å)	1.54184	1.54184
Crystal system	Triclinic	Triclinic
Space group	P-1	P-1
a (Å)	7.9282(2)	7.8658(3)
b (Å)	13.3615(4)	13.1568(5)
c (Å)	14.0733(4)	13.8695(4)
α (°)	92.407(2)	89.380(3)
β (°)	78.061(2)	76.884(3)
γ (°)	77.177(2)	80.584(3)
V (Å^3)	1416.15(7)	1378.54(9)
Z	2	2
D_{calc} (g.cm^{-3})	1.280	1.314
μ (mm^{-1})	0.65	0.67
F(000)	566	566
ϑ_{min}, ϑ_{max} (°)	4.5, 75.7	4.6, 75.9
Refl. Collected	24690	22247
Refl. Indep., R_{int}	5778, 0.051	5604, 0.033
Refl. Observed	4554	4634
Ref. param., restr.	387, 4	380, 0
GOF	1.81	1.71
R_1 [$I > 3\sigma(I)$]	0.048	0.040
wR_2 [$I > 3\sigma(I)$]	0.130	0.108
R_1 (all data)	0.058	0.047
wR_2 (all data)	0.138	0.112
$\Delta\rho_{min}$, $\Delta\rho_{max}$ (e$^-$.Å^{-3})	-0.28, 0.25	-0.27, 0.27

Table S2 Selected bond lengths in crystal structures of **1**.

Phase	**HT**	**LT**
X–Y	X–Y (Å)	X–Y (Å)
C1a–C2a	1.434(2)	1.4413(17)
C1a–C6a	1.437(2)	1.4433(18)
C1a–C7a	1.3947(17)	1.3898(14)
C2a–C3a	1.3526(17)	1.3537(14)
C3a–C4a	1.4329(19)	1.4404(17)
C4a–C5a	1.438(2)	1.4444(17)
C4a–C10a	1.3879(16)	1.3868(14)
C5a–C6a	1.3497(16)	1.3545(14)
C7a–C8a	1.424(2)	1.4322(18)
C7a–C9a	1.423(2)	1.4314(17)
C10a–C11a	1.427(2)	1.4325(17)
C10a–C12a	1.423(2)	1.4294(18)
C1b–C2b	1.4354(19)	1.4361(16)

C1b–C6b	1.4326(19)	1.4341(17)
C1b–C7b	1.3950(16)	1.4011(14)
C2b–C3b	1.3578(16)	1.3614(14)
C3b–C4b	1.4328(19)	1.4310(17)
C4b–C5b	1.433(2)	1.4349(16)
C4b–C10b	1.4006(17)	1.4071(14)
C5b–C6b	1.3540(16)	1.3613(14)
C7b–C8b	1.422(2)	1.4263(17)
C7b–C9b	1.424(2)	1.4279(17)
C10b–C11b	1.419(2)	1.4245(17)
C10b–C12b	1.424(2)	1.4247(18)

Table S3 The shortest C···C interactions between anion-radicals in **1**.

Phase	**HT**		**LT**
C(x)···C(y)	C(x)···C(y) (Å)	C(x)···C(y)	C(x)···C(y) (Å)
C9a···C10a^{i}	3.545(2)	C9a···C10a^{i}	3.4324(15)
C10a···C4b	3.2060(17)	C1a···C7b	3.1846(14)
C2b···C6b^{ii}	3.3985(18)	C1b···C3b^{ii}	3.2581(15)

Symmetry codes: (*i*) -*x*, 2-*y*, 1-*z*; (*ii*) 1-*x*, 1-*y*, 1-*z*.

Table S4 Possible weak hydrogen bonds in **1** at 250 K (HT).

D-H···A	D-H (Å)	H···A (Å)	D···A (Å)	∠(D-H···A) (°)
C3a- H1c3a···N2a^{i}	0.9600(14)	2.5438(17)	3.2224(22)	127.770(88)
C3b- H1c3b ···N2b^{i}	0.9600(14)	2.7553(16)	3.3868(22)	123.987(83)
C5a^{i}- H1c5a^{i}···N3a	0.9600(14)	2.8127(15)	3.4098(21)	121.154(87)
C6a^{i}- H1c6a^{i}···N3a	0.9599(14)	2.7263(16)	3.3713(22)	125.120(89)
C5b^{i}- H1c5b^{i}···N3b	0.9600(14)	2.8407(15)	3.4271(21)	120.318(87)
C6b^{i}- H1c6b^{i}···N3b	0.9600(14)	2.7598(16)	3.3868(22)	123.597(86)
C1c^{ii}-H1c1c^{ii}···N1a	0.9599(14)	2.6644(15)	3.3829(20)	132.017(101)
C1c^{iii}- H1c1c^{iii}···N1a^{i}				
C5c^{iv}-H1c5c^{iv}···N3b	0.9599(14)	2.5428(16)	3.3416(43)	140.730(205)
C5c^{v}-H1c5c^{v} ···N3b^{i}				
*C5c^{iv}-*H2c5c^{iv}···N3b	0.9603(96)	2.4877(16)	3.3511(95)	149.560(512)
*C5c^{v}-*H2c5c^{v} ···N3b^{i}				
C4c-H1c4c···N4b	0.9599(18)	2.3253(19)	3.4038(28)	138.452(113)
C4c^{i}-H1c4c^{i}···N4b^{i}				
*C5c-*H1c5c···N4b	0.9604(83)	2.5176(15)	3.3275(69)	142.011(426)
*C5c^{i}-*H1c5c^{i}···N4b^{i}				
C8c^{vi}-H1c8c^{vi}···N4b	0.9599(28)	2.7572(15)	3.6311(31)	151.719(159)
C8c^{iv}-H1c8c^{iv}···N4b^{i}				

Symmetry codes: (*i*) 1+*x*, *y*, *z*; (*ii*) -1+*x*, 1+*y*, 1+*z;* (*iii*) *x*, 1+*y*, 1+z; (*iv*) 2-*x*, 1-*y*, -z; (*v*) 3-*x*, 1-*y*, -z; (*vi*) 1-*x*, 1-*y*, -z. *position occupied with 0.335 probability.

Table S5 Possible weak hydrogen bonds in **1** at 95 K (LT).

D-H···A	D-H (Å)	H···A (Å)	D···A (Å)	∠(D-H···A) (°)
C2a- H1c2a···N2a^{i}	0.9600(12)	2.6566(11)	3.2637(17)	121.594(72)
C3a- H1c3a···N2a^{i}	0.9600(12)	2.5495(12)	3.2136(17)	126.410(71)
C2b- H1c2b ···N2b^{i}	0.9599(12**)**	2.6739(11)	3.3032(17)	123.586(71)
C3b- H1c3b ···N2b^{i}	0.9600(12)	2.6447(12)	3.2920(17)	125.125(71)
C5a^{i}- H1c5a^{i}···N3a	0.9601(12)	2.7052(11)	3.3422(17)	124.343(71)
C6a^{i}- H1c6a^{i}···N3a	0.9600(12)	2.7226(12)	3.3537(17)	123.871(71)
C5b^{i}- H1c5b^{i}···N3b	0.9599(12)	2.6952(11)	3.3328(17)	124.383(71)
C6b^{i}- H1c6b^{i}···N3b	0.9600(12)	2.7082(11)	3.3419(17)	124.058(71)
C1c^{ii}-H1c1c^{ii}···N1a	0.9600(11)	2.7053(11)	3.3596(14)	125.929(71)
C1c^{iv}- H1c1c^{iv}···N1a^{i}				
C1c^{iii}-H1c1c^{iii}···N1a	0.9600(11)	2.7383(11)	3.3609(16)	123.157(74)
C1c^{v}- H1c1c^{v}···N1a^{i}				
C8c^{vi}-H3c8c^{vi}···N2b	0.9600(13)	2.7456(11)	3.5623(17)	143.362(76)
C8c^{iii}-H3c8c^{iii}···N2b^{i}				
C5c^{vii}-H2c5c^{vii}···N3b	0.9599(13)	2.5732(11)	3.4213(16)	147.404(76)
C5c^{viii}-H2c5c^{vii}···N3b^{i}				
C4c-H1c4c···N4b	0.9599(12)	2.4902(12)	3.1978(17)	130.469(74)
C4c^{i}-H1c4c^{i}···N4b^{i}				
C8c^{ix}-H1c8c^{ix}···N4b	0.9601(13)	2.6410(11)	3.4939(16)	148.211(78)
C8c^{vii}-H1c8c^{vii}···N4b^{i}				

Symmetry codes: (*i*) 1+*x*, *y*, *z*; (*ii*) -1+*x*, 1+*y*, 1+*z;* (*iii*) 1-*x*, 1-*y*, 1-z; (*iv*) *x*, 1+*y*, 1+z; (*v*) 2-*x*, 1-*y*, 1-z; (*vi*) *x*, 1-*y*, 1-z; (*vii*) 2-*x*, 1-*y*, -z; (*viii*) 3-*x*, 1-*y*, z; (*ix*) 1-*x*, 1-*y*, -z;.

Table S6 Analysis of the TCNQ bond distances and correlation between bond length and charge of TCNQ molecules in **1** using the Kistenmacher relationship.

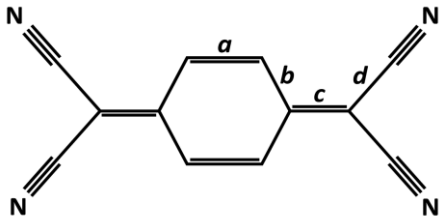

	a	*b*	*c*	*d*	*b - c*	*c - d*	*c/(b + d)*	*Q*
TCNQ^{0}	1.345	1.448	1.374	1.441	0.074	-0.067	0.476	0.001
TCNQ$^{-0.5}$	1.354	1.434	1.396	1.428	0.040	-0.032	0.488	0.500
TCNQ^{-}	1.374	1.423	1.420	1.416	0.003	0.004	0.500	0.999
250 K								
TCNQ A	1.354	1.433	1.399	1.423	0.035	-0.024	0.490	0.571
TCNQ B	1.351	1.433	1.391	1.425	0.042	-0.033	0.487	0.451
95 K								
TCNQ A	1.362	1.433	1.405	1.426	0.028	-0.022	0.492	0.637
TCNQ B	1.355	1.442	1.388	1.432	0.057	-0.044	0.483	0.295

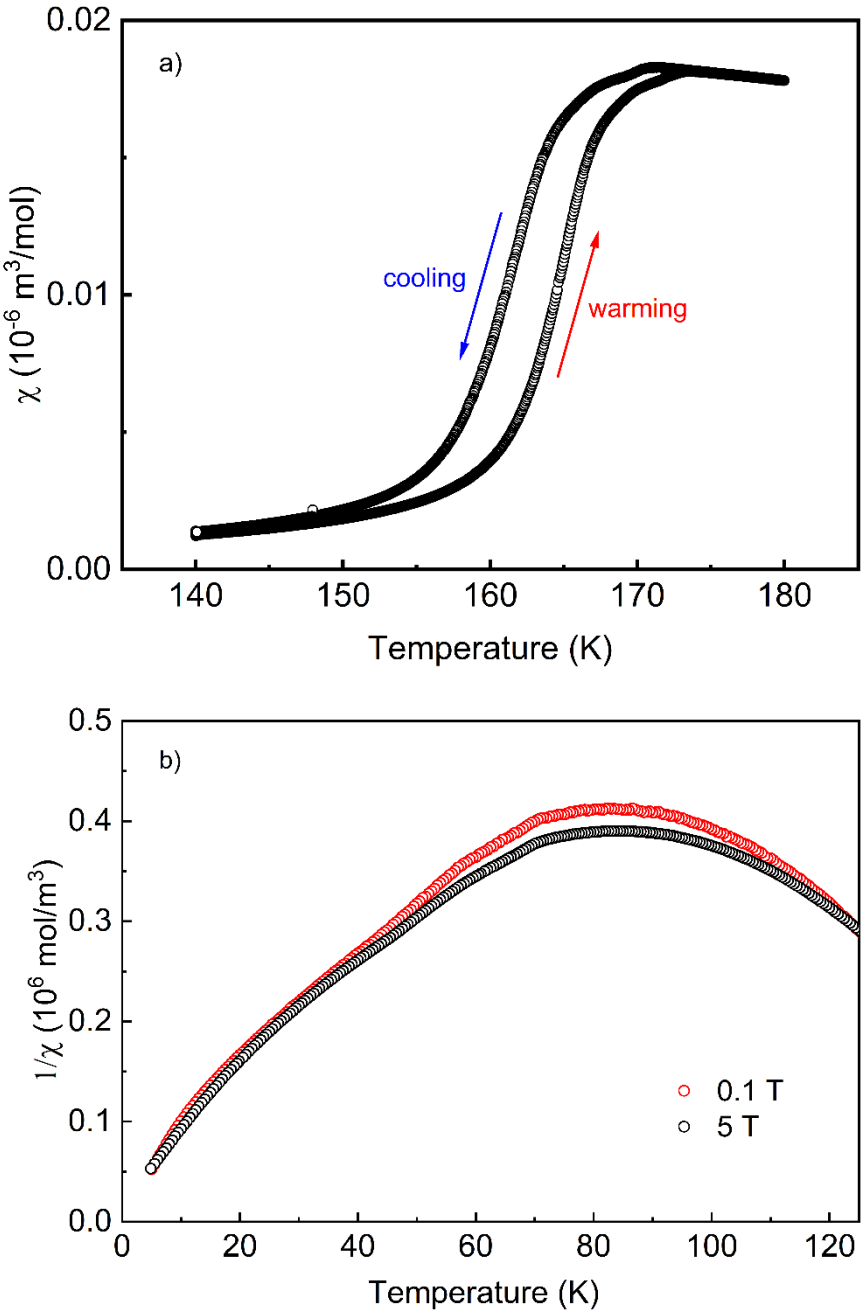

Figure S1 a) The magnetic response of **1** during thermal cycling in the magnetic field of 5 T. b) Inverse susceptibility (calculated as M/H) measured in cooling mode in the LT phase.

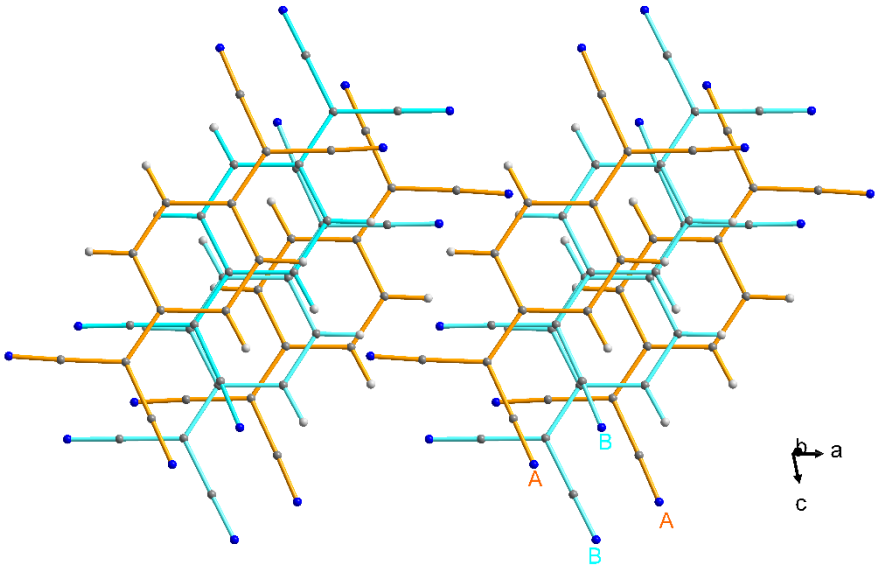

Figure S2 View of the TCNQ stacks along the *b**-axis (perpendicular to the *ac*-plane) as used for the measurements of resistivity.

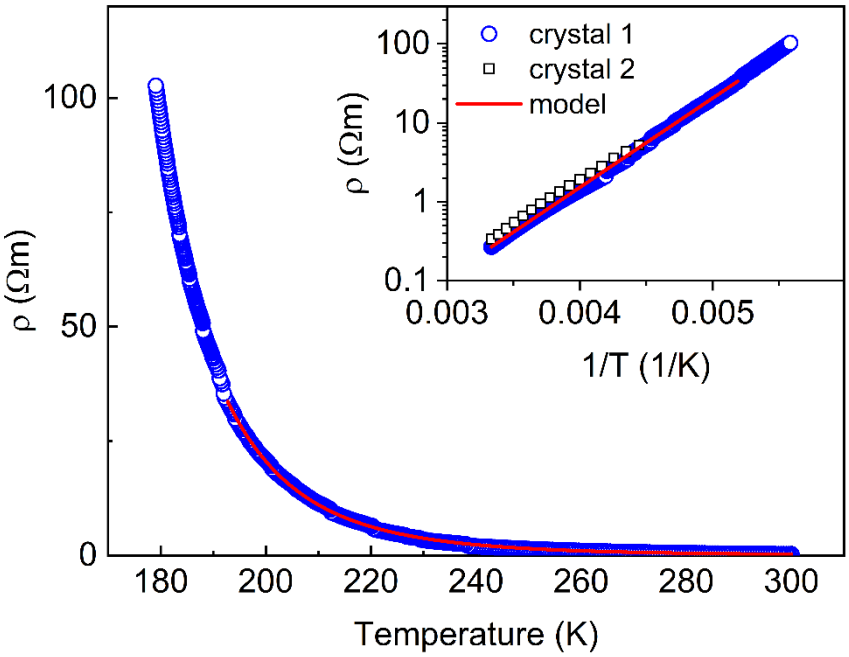

Figure S3 Temperature dependence of the resistivity of a crystal of **1** (blue and black open symbols for two different crystals in a similar measurement geometry), measured in a cooling cycle, showing semiconducting behaviour in the HT phase (red solid line). The inset shows the resistivity in the Arrhenius plot.

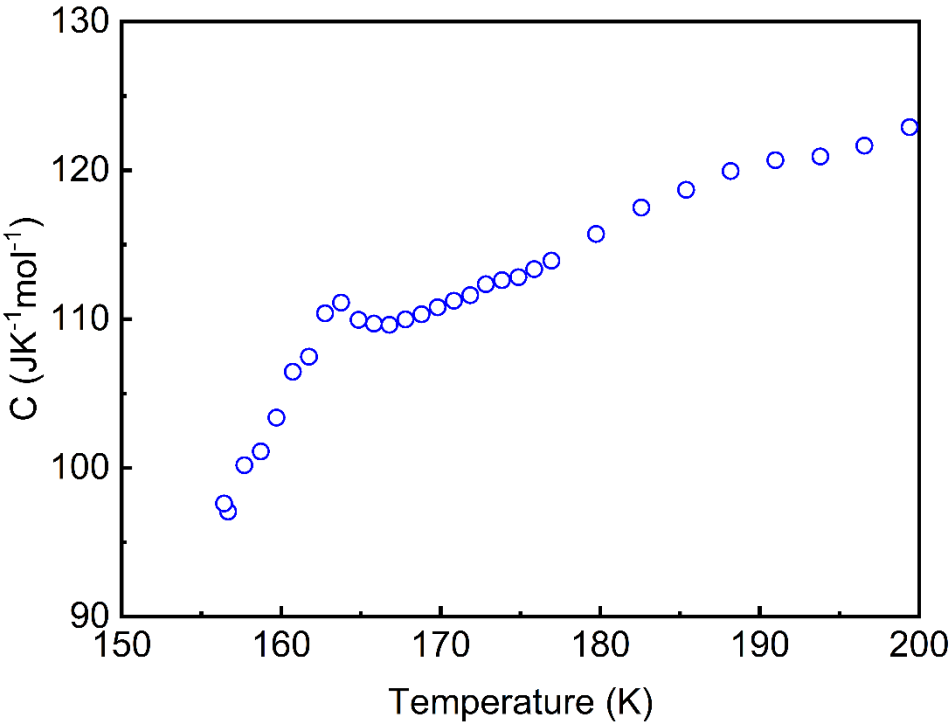

Figure S4 Temperature dependence of specific heat of **1** in zero magnetic field measured in a cooling cycle.

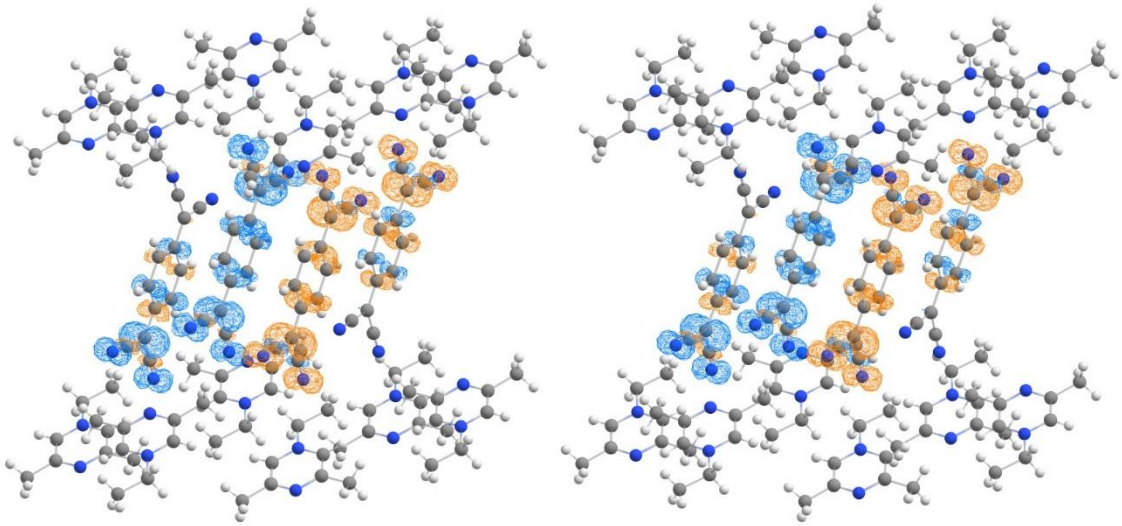

a) BS1 b) BS2

Figure S5 The spin density of the BS states of two large model molecules (lm, Table 3) with four TCNQ anion radicals surrounded by twelve nearest cations extracted from the crystal structure of **1** obtained at 95 K. The blue and orange colours of the spin density distribution correspond to the two opposite spin polarisations (isovalue 0.002). Exchange interactions J_1 (corresponding to AB-BA interaction, BS1) and J_2 (corresponding to BA-AB interaction, BS2) were calculated using the BS DFT approach.

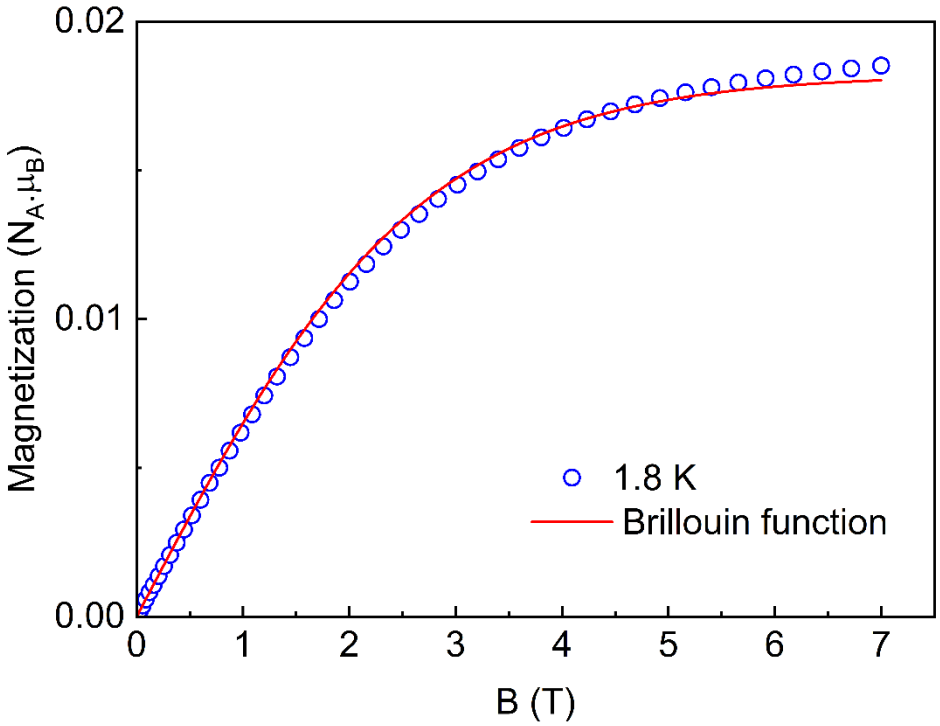

Figure S6 Field dependence of magnetisation of **1** at 1.8 K (blue open symbols); the solid red line represents the fit of the Brillouin function taking into account the existence of paramagnetic spins with concentration of ρ = 0.018.